Research Article

A DFT-based Analysis of Metals Adsorption on Chitosan Monomer

Malinee Promkatkaew[1*], Sunan Kitjaruwankul[1], Supaporn Baiya[1], Suree Tongwanichniyom[1], Pornthip Boonsri[2], and Supa Hannongbua[3]

_____

ABSTRACT

The generation of waste electrical and electronic equipment (WEEE or E-waste) has been noted as an increasing category of waste. In this work, the density functional theory (DFT) was used to investigate the adsorption process between chitosan (CS) and metals at the B3LYP level with 6-31G(d,p) and LANL2DZ basis sets. The effect of solvent was included using the polarizable continuum model (PCM) consisting of water. Ag^+, As^{3+}, Ba^{2+}, Be^{2+}, Cd^{2+}, Co^{2+}, Cr^{3+}, Cu^{2+}, Hg^{2+}, Li^+, Mn^{2+}, Ni^{2+}, Pb^{2+}, Pd^{2+}, Sb^{3+}, Sn^{2+}, Sr^{2+}, Tl^+, and Zn^{2+} have been selected to be studied because of high impact in E-waste. Different analyses were carried out: adsorption energy, HOMO-LUMO energy gaps, hardness, softness, frontier molecular orbitals, and molecular electrostatic potential (MEP), and all of which are necessary to predict the formation of complexes. The interaction between CS and metal species was shown in almost all cases as covalent partial. In addition, all metals were placed closeer to the nitrogen atom than the oxygen atom of CS because the charge density of the nitrogen is increased in the formation of the Schiff base. Finally, the monomer derived from CS has good stability in water and is, therefore, considered as a good material in the field of environmental pollution.

_____

[1] Faculty of Science at Sriracha, Kasetsart University Sriracha Campus, Chonburi 20230 Thailand

[2] Department of Chemistry, Faculty of Science, Srinakharinwirot University, Bangkok 10110, Thailand

[3] Department of Chemistry, Faculty of Science, Kasetsart University, Bangkok 10903 Thailand

*Corresponding author, email: sfscimlp@ku.ac.th

Introduction

The rapid upgrading of electronic devices and the quickly developing of the electronic information industry have affected in forcing of waste electrical and electronic equipment (widely known as WEEE or E-waste) [1-3]. It is a heterogeneous combination of metallic and non-metallic materials, including plastics, ceramics, copper, precious metals (Au, Ag, Pt, and Pd), heavy metals (Pb, Hg, Cr, and As, etc.), and other typical trace elements (Ni, Co, and Sn) [1, 4]. These toxic metals in the finest fractions might be easily released into the environment and society during the mechanical processing of E-waste, which is particularly dangerous [5, 6]. Therefore, the treatment methods for removing or measuring for maximum allowable limits of those metal ions discharged into the environment are needed to be environmentally friendly. Various conventional methods that have been applied in metal ions removal have some disadvantages in that they are associated with high costs and are less efficient at low metal concentrations [7, 8]. Therefore, the potential of adsorbent materials which originally come from nature, to adsorb metal ions, has attracted immense interest in the development of today's research.

Chitosan (CS) is an excellent biopolymer capable of adsorbing heavy metals, dyes, and proteins, which is cheap and easily available. CS can be easily modified by grafting new functional groups onto the polymer backbone to increase its range of properties and functionalities. It has a large number of both amine and hydroxyl functionalities that are related to an increase in the potential for adsorbing heavy metals and is also a highly hydrophilic material. The advantage of using CS for metal adsorption is that the amino sites of CS are easily protonated in acid media, and the electrostatic forces are often implicated in the initial stages of adsorption [9]. Due to the special structure of CS, it can easily form chelate rings in coordination with metal ions, which accounts for its use as a candidate for wastewater treatment [10, 11].

Computational methods as an effective tool to study the physical and chemical behavior of many systems and molecules covering many fields of applications [12-14]. The density functional theory (DFT) was successfully applied to predict the possible interaction between each metal ion and CS and its derivatives which confirmed that CS is a good adsorbent for divalent metals Hg [15] and Ni, Cu, As, Cd, and Pb [11]. Therefore, considering the potential adsorption of the CS and the problem caused by metals ions, the objective of this work was to do the theoretical study of the interaction of the Ag^+, As^{3+}, Ba^{2+}, Be^{2+}, Cd^{2+}, Co^{2+}, Cr^{3+}, Cu^{2+}, Hg^{2+}, Li^+, Mn^{2+}, Ni^{2+}, Pb^{2+}, Pd^{2+}, Sb^{3+}, Sn^{2+}, Sr^{2+}, Tl^+ and Zn^{2+} metal cations with chitosan monomer.

Methods of Calculations

The adsorption process between chitosan monomer (CS) and metals was investigated by using the density functional theory (DFT) calculations. In this work, Ag^+, As^{3+}, Ba^{2+}, Be^{2+}, Cd^{2+}, Co^{2+}, Cr^{3+}, Cu^{2+}, Hg^{2+}, Li^+, Mn^{2+}, Ni^{2+}, Pb^{2+}, Pd^{2+}, Sb^{3+}, Sn^{2+}, Sr^{2+}, Tl^+, and Zn^{2+} have been selected as the metals to be studied because of high impact in E-waste [1, 2]. All calculations were carried out at the B3LYP [16, 17] functional with the 6-31G(d,p) basis set for the H, C, N, and O atoms while the Los Alamos effective core potential (ECP) [18] included relativistic effects plus double atomic orbitals at the

LANL2DZ basis set was selected for the metal atoms. The effect of solvent was studied using the polarizable continuum model (PCM) [19] consisting of water using a dielectric constant (ε) as 78.3553.

The interaction process was quantified by equation 1.

$$E_{int} \quad = \quad E_{complex} - [E_{ligand} + E_{metal\ ion}] \tag{1}$$

Where E_{int} is the interaction energy, $E_{complex}$ corresponds to the energy of the complex (polymer + ion), and E_{ligand} and $E_{metal\ ion}$ are the energy of the polymer and the metal ion isolated, respectively.

Gibbs energy was calculated by equation 2.

$$\Delta G \quad = \quad \sum G_P - \sum G_R \tag{2}$$

Where G_P and G_R are the Gibbs Energy at 298 K for products and reagents, respectively.

The highest occupied molecular orbital (HOMO: E_H) and lowest unoccupied molecular orbital (LUMO: E_L) energies were employed to obtain the reactivity indices: chemical hardness (η) and softness (S). Taking into account the Koopmans theorem [20], the indices can be determined by equation 3 and 4.

$$\eta \quad = \quad (E_L - E_H) \ / \ 2 \tag{3}$$

$$S \quad = \quad 1 \ / \ \eta \tag{4}$$

All calculations were performed using the Gaussian 09 program [21].

Results and Discussion

To understand the adsorption of the metal ions into the polymer matrix, a simple model was applied to mimic the real system and to reduce the computational time. Hence, only one monomeric unit of CS has been selected for the adsorption of the metal ions in this study. In the present work, 19 metal ions including 3 monovalent, 13 divalent, and 3 trivalent metal cations have been selected from metals in E-waste [1, 2].

Structural analysis

The electronic interaction energies (E_{int}), Gibbs energy (ΔG), and total dipole moment (TDM) of CS and CS-metal complexes are shown in Table 1. The obtained E_{int} of CS structure interacting with metals was determined to be -0.405 to -20.000 eV. In addition, the difference in the oxidation number of metal ions was considered as the key point for the adsorption process. The E_{int} values showed that the most stable complexes were ranked by trivalent, divalent, and monovalent metal cations, respectively. Besides that, Ag^+, Cu^{2+}, and As^{3+} presented the highest values of energy variation, -2.408, -9.179, and -20.000 eV for monovalent, divalent, and trivalent metal cations, respectively. It indicated that the trivalent metal cations adsorbed to CS showed the most stable metal-CS complex with the highest E_{int} values. ΔG showed the same tendency of electronic interaction energies as -0.202 to -0.512 eV which was revealed as a spontaneous process. Furthermore, the TDM cloud is correlated with the reactivity of a given compound. TDM of CS was calculated to be 4.642 Debye, while in the presence of metals was increased from 4.799 to 23.292 Debye, which means that CS was affected by metals. CS could interact

with all studied metals and have more ability to interact with Ba^{2+}, Sr^{2+}, and Cr^{3+} which have the highest TDM value.

The optimized structures of CS and CS-metal complexes and bond distances between metals and nitrogen atoms or between metal and oxygen atoms in Å are displayed in Figure 1. The interaction between CS monomer and metal species was shown in almost all cases as covalent partial. In addition, all metals were placed close to the nitrogen atom than the oxygen atom of CS, because the charge density of the nitrogen is increased in the formation of the Schiff base. The metal-nitrogen distances of all CS-metal complexes are 1.544 to 2.768 Å, whiles, the metal-oxygen distances are 1.674 to 3.237 Å. In addition, the higher negative E_{int} values resulted in shorter distances between metal-nitrogen and metal-oxygen interaction. Whereas the higher negative energy of ΔG gives the longer distances between metal-nitrogen and metal-oxygen.
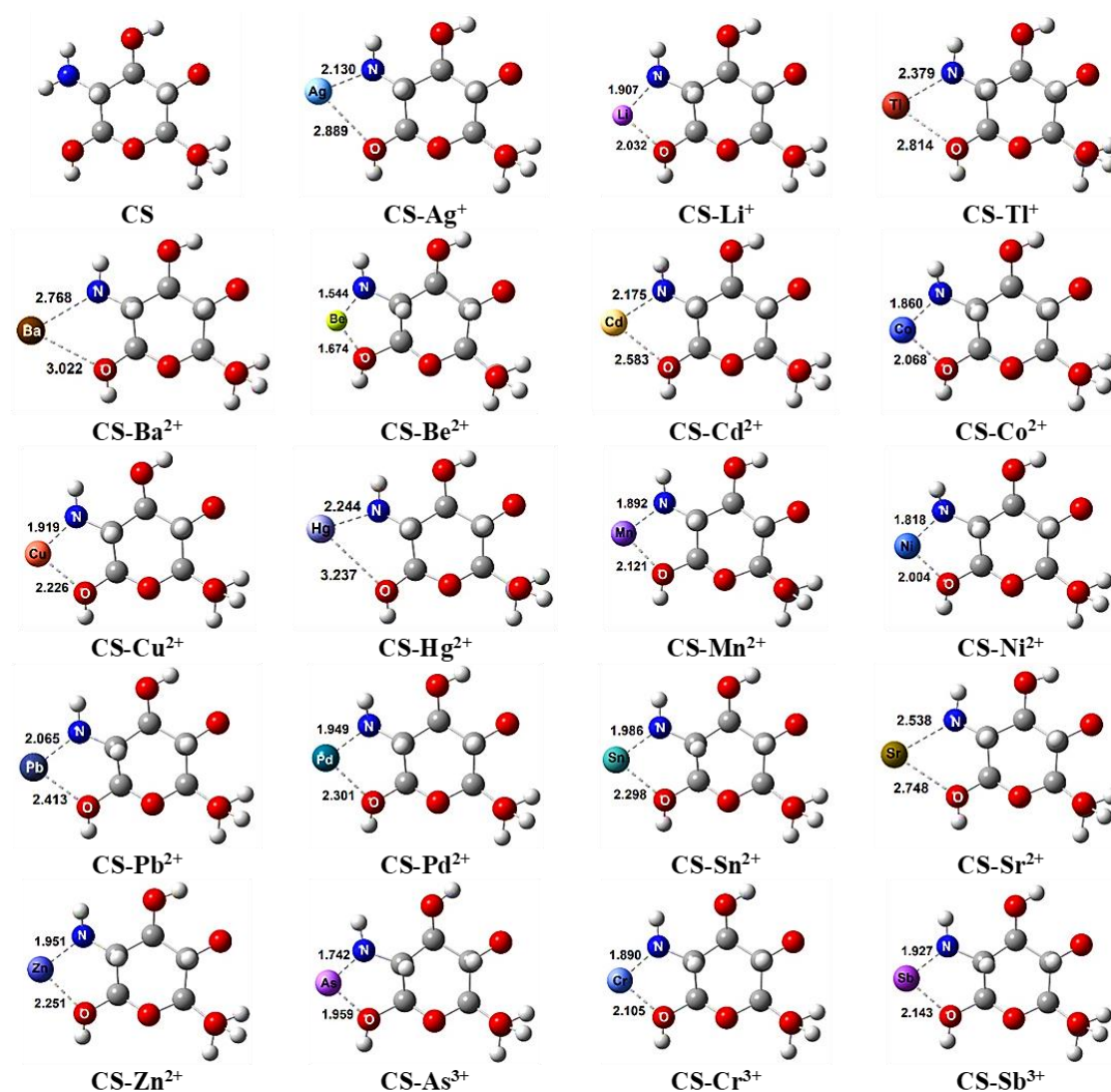

Figure 1 Optimized structures of CS and CS-metal complexes were calculated using the PCM-B3LYP/6-31G(d,p)/LANL2DZ in water. Bond distances are shown in Å.

Table 1 Electronic interaction energies (E_{int}), Gibbs energy (ΔG), and total dipole moment (TDM) of CS and CS-metal complexes. The values were obtained from the PCM-B3LYP/6-31G(d,p)/LANL2DZ in water.

Structure	E_{int} (eV)	ΔG (eV)	TDM (Debye)
CS	-	-	4.642
CS-Ag$^+$	-2.408	-0.467	4.799
CS-Li$^+$	-1.535	-0.333	7.488
CS-Tl$^+$	-1.820	-0.512	6.002
CS-Ba^{2+}	-0.405	-0.511	24.931
CS-Be^{2+}	-7.365	-0.202	14.305
CS-Cd^{2+}	-2.537	-0.420	16.550
CS-Co^{2+}	-6.225	-0.395	12.804
CS-Cu^{2+}	-9.179	-0.439	9.288
CS-Hg^{2+}	-2.366	-0.458	13.735
CS-Mn^{2+}	-6.194	-0.350	14.998
CS-Ni^{2+}	-7.290	-0.324	11.375
CS-Pb^{2+}	-6.143	-0.403	7.604
CS-Pd^{2+}	-7.646	-0.380	8.728
CS-Sn^{2+}	-7.686	-0.353	7.830
CS-Sr^{2+}	-1.230	-0.488	23.593
CS-Zn^{2+}	-3.603	-0.372	16.047
CS-As^{3+}	-20.000	-0.345	14.484
CS-Cr^{3+}	-18.904	-0.352	23.292
CS-Sb^{3+}	-14.811	-0.347	14.015

Chemical index parameters

The HOMO-LUMO energy gap is a characteristic observation of molecules. It can predict the reactivity, stability of complexes formed, and conductance of molecules. Energies of the HOMO (E_H) and LUMO (E_L) orbitals, HOMO-LUMO bandgap (ΔE), hardness (η), and softness (S) for CS and CS-metal complexes of the CS are given in Table 2. The energy diagram of HOMO and LUMO orbitals of CS and CS structure interacting with metals are shown in Figures 2, 3 and 4, for monovalent, divalent, and trivalent metal cations, respectively.

The difference between LUMO and HOMO (E_L-E_H) is taken as ΔE, expressed in eV. HOMO-LUMO energy gaps of CS were calculated to be 8.40 eV, while in the presence of metals were decreased to 2.08 - 5.40 eV. The obtained results revealed that Ag$^+$, Pd^{2+}, and As^{3+} represented as the best ΔE values for the monovalent, divalent, and trivalent metal cations at 3.42, 2.93, and 2.08 eV, respectively.

The calculated value of the η = 4.50 eV and S = 0.24 eV leads to the strengthening of the stability of CS. For CS-metal complexes, the η value is decreased from 1.04 to 2.67 eV, whereas the S value is increased from 0.37 to 0.96 eV. After analyzing the results, it is possible to consider that the monomer is a relatively hard compound. Ag^+, Pd^{2+}, and As^{3+} cations presented softness that tends to have a favorable interaction with the CS monomer corresponding to the HOMO-LUMO energy gaps.

In the CS molecule, the calculated energy value of HOMO is -6.64 eV, and the energy of LUMO is 1.77 eV. The HOMO of CS shows a delocalization on the aromatic ring and the base group of Schiff near the amine group. In this sense, it is suggested that not only the amine group can establish the interaction with the metal ions but also the aromatic ring. While the LUMO of CS shows a delocalization on the aromatic ring near hydroxyl and methyl groups. For all CS-metal complexes, the π electrons at HOMO are mainly localized on the conjugation along the molecule near the amine group whereas the LUMO is mainly distributed on the metal ions.

Table 2 Energies of the LUMO (E_L) and HOMO (E_H) orbitals, HOMO-LUMO band gap (ΔE), hardness (η), and softness (S) for CS and CS-metal complexes. The calculations were performed using the PCM-B3LYP/6-31G(d,p)/LANL2DZ in water. All values are reported in eV.

| Structure	E_L	E_H	ΔE	η	S
CS	1.77	-6.64	8.41	4.20	0.24
CS-Ag$^+$	-1.47	-4.89	3.42	1.71	0.58
CS-Li$^+$	0.16	-4.07	4.23	2.11	0.47
CS-Tl$^+$	-0.49	-4.51	4.01	2.01	0.50
CS-Ba^{2+}	-0.07	-3.49	3.42	1.71	0.59
CS-Be^{2+}	-1.23	-6.62	5.40	2.70	0.37
CS-Cd^{2+}	-1.61	-5.35	3.73	1.87	0.54
CS-Co^{2+}	-3.21	-6.37	3.16	1.58	0.63
CS-Cu^{2+}	-1.99	-7.32	5.33	2.67	0.37
CS-Hg^{2+}	-1.98	-5.69	3.71	1.85	0.54
CS-Mn^{2+}	-1.79	-5.72	3.93	1.97	0.51
CS-Ni^{2+}	-3.59	-6.71	3.11	1.56	0.64
CS-Pb^{2+}	-2.31	-6.82	4.51	2.26	0.44
CS-Pd^{2+}	-3.83	-6.76	2.93	1.47	0.68
CS-Sn^{2+}	-2.53	-7.19	4.66	2.33	0.43
CS-Sr^{2+}	-0.31	-3.85	3.55	1.77	0.56
CS-Zn^{2+}	-1.56	-5.69	4.12	2.06	0.48
CS-As^{3+}	-5.72	-7.80	2.08	1.04	0.96
CS-Cr^{3+}	-4.90	-7.58	2.68	1.34	0.75
CS-Sb^{3+}	-5.33	-7.73	2.41	1.20	0.83
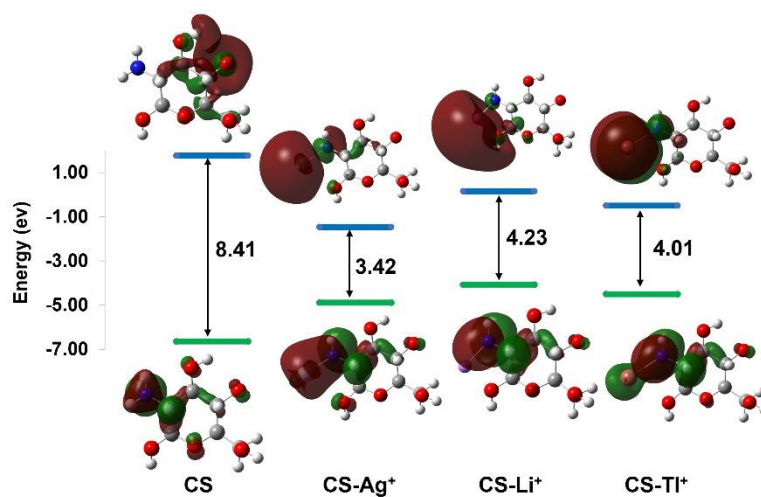
Figure 2 Energy diagram of HOMO and LUMO orbitals (in eV) of CS and CS-monovalent metal cation complexes.
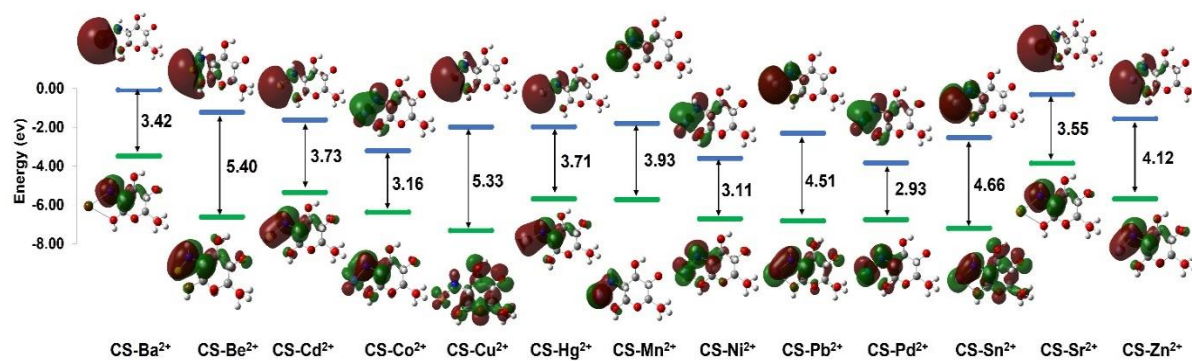

Figure 3 Energy diagram of HOMO and LUMO orbitals (in eV) of CS-divalent metal cation complexes.
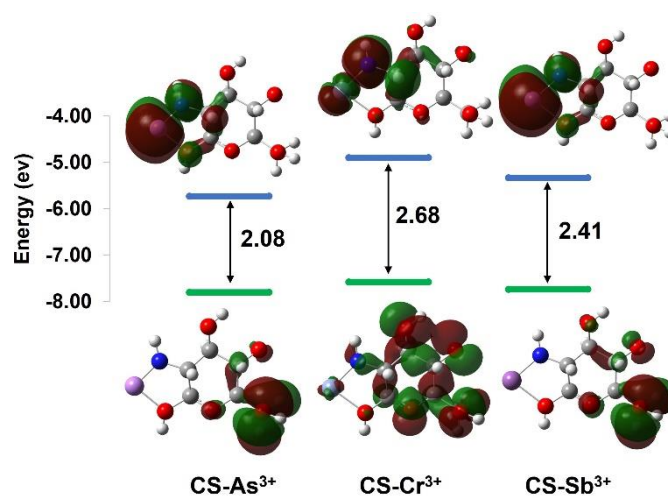

Figure 4 Energy diagram of HOMO and LUMO orbitals (in eV) of CS-trivalent metal cation complexes.

Molecular electrostatic potential

The molecular electrostatic potential (MEP) provides information on the local reactivity of the molecules, due to the density of electrons. Using the analysis of these MEPs can predict the possible sites or the reaction mechanisms of a complex formation. The reactivity of the molecule can be observed through MEP, in the regions with the most intense colors, orange or red indicates partially negative regions and blue indicates a partially positive region. Figure 5 shows the MEP of CS and CS structure interacting with metals as well as the colorings related to the charge density. The adsorption regions between CS-metal complexes are the main interest which must have red staining as the negative charge density, to the positive charge density.

Two regions of the CS molecule present both amine and hydroxyl functionalities. However, it is necessary to disregard the upper region of the polymer because it will be conjugated with the rest of the monomeric units. Thus, in the upper part, the interaction with the metal ions will be less favorable due to the steric effect that the other groups can interfere with. In the left part of the CS monomer, the amine and hydroxyl groups, which compose the other region of interest, concentrate a high density of negative charge due to the oxygen and nitrogen atoms. These regions are very electronegative and sensible to reactions or interactions involving electrophiles. Whereas all the CS-metal complexes are positive charge density, they have a blue coloration. Therefore, based on the MEP investigation, suggests the possibility to infer the possible interaction site of the CS monomer with the metal cation.
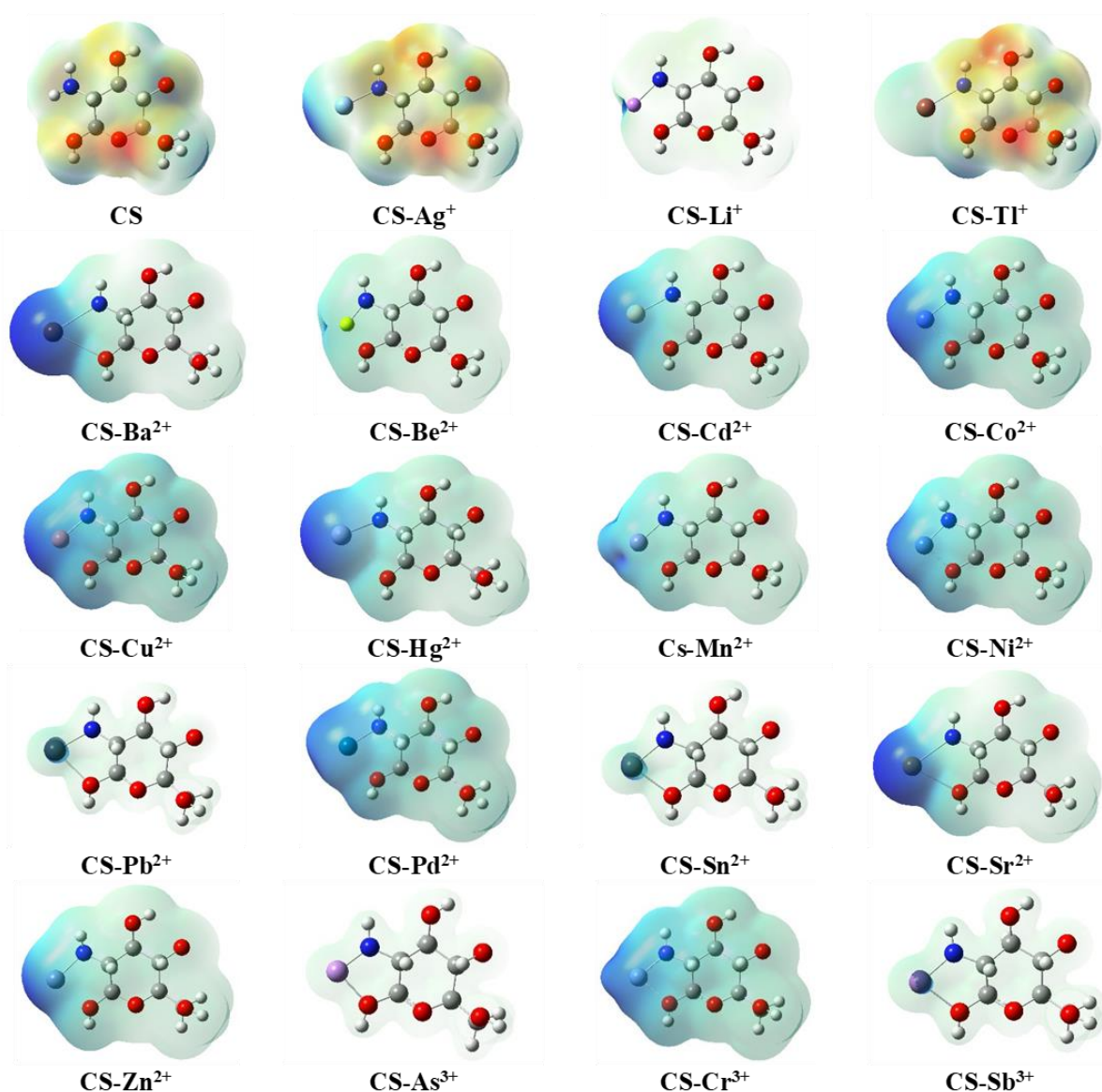
Figure 5 Molecular electrostatic potential (MEP) of CS and CS structure interacting with metals.

Conclusions

DFT calculations were investigated for CS ability to complex with Ag^+, As^{3+}, Ba^{2+}, Be^{2+}, Cd^{2+}, Co^{2+}, Cr^{3+}, Cu^{2+}, Hg^{2+}, Li^+, Mn^{2+}, Ni^{2+}, Pb^{2+}, Pd^{2+}, Sb^{3+}, Sn^{2+}, Sr^{2+}, Tl^+ and Zn^{2+} metal ions. The electronic interaction energies (E_{int}) values showed that the most stable complexes were Ag > Tl > Li of CS-monovalent metal cations. For CS-divalent metal cations, the E_{int} values were in the order Cu > Sn > Pd > Be > Ni > Co > Mn > Pb > Zn > Cd > Hg > Sr > Br. Finally, the E_{int} values showed the most stable complexes were As > Cr > Sb of CS-trivalent metal cations. Moreover, the trivalent metal cations adsorbed to CS showed the most stable metal-CS complex with the highest E_{int} values. In the presence of metals, it was found that HOMO-LUMO energy gaps decreased, while the total dipole moment increased. The monomer derived from CS has good stability in water and is therefore considered as a good material in the field of environmental pollution.

Acknowledgments

References

1. Robinson BH. E-waste: An assessment of global production and environmental impacts. Sci Total Environ. 2009; 408(2):183-91.

2. Willner J, Fornalczyk A, Jablonska-Czapla M, Grygoyc K, Rachwal M. Studies on the content of selected technology critical elements (germanium, tellurium and thallium) in electronic waste. Materials. 2021;14(13):3722.

3. Marinello S, Gamberini R. Multi-criteria decision making approaches applied to waste electrical and electronic equipment (WEEE): A comprehensive literature review. Toxics. 2021;9(1):13.

4. Chen M, Avarmaa K, Taskinen P, Klemettinen L, Michallik R, O'Brien H, et al. Handling trace elements in WEEE recycling through copper smelting-an experimental and thermodynamic study. Miner Eng. 2021;173:107189.

5. Sepúlveda A, Schluep M, Renaud FG, Streicher M, Kuehr R, Hagelüken C, et al. A review of the environmental fate and effects of hazardous substances released from electrical and electronic equipments during recycling: Examples from China and India. Environ Impact Assess Rev. 2010;30(1):28-41.

6. Song Q, Li J. A review on human health consequences of metals exposure to e-waste in China. Environ Pollut. 2015;196:450-61.

7. Gurgel LVA, Júnior OK, Gil RPdF, Gil LF. Adsorption of Cu(II), Cd(II), and Pb(II) from aqueous single metal solutions by cellulose and mercerized cellulose chemically modified with succinic anhydride. Bioresour Technol. 2008;99(8):3077-83.

8. Cherono F, Mburu N, Kakoi B. Adsorption of lead, copper and zinc in a multi-metal aqueous solution by waste rubber tires for the design of single batch adsorber. Heliyon. 2021;7(11):e08254.

9. Das N. Recovery of precious metals through biosorption- A review. Hydrometallurgy. 2010;103(1):180-9.

10. Liu B, Wang D, Yu G, Meng X. Adsorption of heavy metal ions, dyes and proteins by chitosan composites and derivatives-A review. J Ocean Uni China. 2013;12:500-8.

11. Menazea AA, Ezzat HA, Omara W, Basyouni OH, Ibrahim SA, Mohamed AA, et al. Chitosan/graphene oxide composite as an effective removal of Ni, Cu, As, Cd and Pb from wastewater. Comput and Theor Chem. 2020;1189:112980.

12. Promkatkaew M, Boonsri P, Hannongbua S. Structural and spectroscopic properties of metal complexes with Ruhemann's purple compounds calculated using density functional theory. Key Eng Mater. 2019;824:204-11.

13. Ribeiro IHS, Reis DT, Pereira DH. A DFT-based analysis of adsorption of Cd^{2+}, Cr^{3+}, Cu^{2+}, Hg^{2+}, Pb^{2+}, and Zn^{2+}, on vanillin monomer: a study of the removal of metal ions from effluents. J Mol Model. 2019;25(9):267.

14. Promkatkaew M, Suramitr S, Karpkird T, Ehara M, Hannongbua S. DFT/TD-DFT investigation on the photoinduced electron transfer of diruthenium and viologen complexes. J Lumin. 2020;222:117121.

15. Hassan B, Rajan VK, Mujeeb VMA, K M. A DFT based analysis of adsorption of Hg^{2+} ion on chitosan monomer and its citralidene and salicylidene derivatives: Prior to the removal of Hg toxicity. Int J Biol Macromol. 2017;99:549-54.

16. Becke AD. Density-functional thermochemistry. III. The role of exact exchange. J Chem Phys. 1993;98(7):5648-52.

17. Lee C, Yang W, Parr RG. Development of the Colle-Salvetti correlation-energy formula into a functional of the electron density. Phys Rev B. 1988;37(2):785-9.

18. Hay PJ, Wadt WR. Ab initio effective core potentials for molecular calculations. Potentials for the transition metal atoms Sc to Hg J Chem Phys. 1985;82(1):270-283.

19. Mennucci B, Tomasi J, Cammi R, Cheeseman JR, Frisch MJ, Devlin FJ, et al. Polarizable continuum model (PCM) Calculations of solvent effects on optical rotations of chiral molecules. J Chem Phys. A. 2002;106(25):6102-13.

20. Chong DP, Westwood NPC, Langhoff SR. Methyl- and dimethylketene: He I photoelectron spectra and vertical ionization potentials calculated by using perturbation corrections to Koopmans' theorem. J Chem Phys. 1984;88(8):1479-81.

21. Frisch MJ, Trucks GW, Schlegel HB, Scuseria GE, Robb MA, Cheeseman JR, et al. Gaussian 16 Rev. C.01. Wallingford, CT. 2016.